

# Non-ideal adsorption of divalent cations on a Langmuir monolayer: A theoretical model for predicting the composition of the resulting Langmuir–Blodgett films

M. Elena Díaz<sup>a</sup>, Ramón L. Cerro<sup>b</sup>, Francisco J. Montes<sup>a,\*</sup>, Miguel A. Galán<sup>a</sup>

<sup>a</sup> Department of Chemical Engineering, University of Salamanca, Plaza de los Caídos 1-5, 37008 Salamanca, Spain

<sup>b</sup> Department of Chemical and Materials Engineering, University of Alabama in Huntsville, Huntsville, AL 35899, USA

Received 9 October 2006; received in revised form 18 December 2006; accepted 18 December 2006

## Abstract

The Langmuir–Blodgett (LB) technique has emerged as an alternative method to carry out a wide range of operations in different areas. LB films containing long-chain carboxylic acids and divalent metallic cations have important applications in the semiconductor industry, among others. In this paper, the chemical composition of LB films is predicted based on an electrochemical model that improves and completes previous efforts in this area. The model presented here constitutes an essential tool for the optimization of the experimental technique. Besides other features, the model predicts the concentration of the four species present at the interface ( $\text{RH}$ ,  $\text{R}^-$ ,  $\text{RM}^+$  and  $\text{R}_2\text{M}$ ) and it allows a realistic calculation of the equilibrium constants ( $K_{\text{RM}^+}$  and  $K_{\text{R}_2\text{M}}$ ) for the formation of the complexes between the carboxylic acid and the cation ( $\text{RM}^+$  and  $\text{R}_2\text{M}$ ) based on a compilation of experimental data regarding the composition of the LB monolayers deposited on a solid substrate. In contrast with previous models, the present model does not constrain the possibility of the formation of complexes containing one and/or two  $\text{RCOO}$ -chains on the surface of the original Langmuir monolayer and it includes the non-ideal mixing behavior of the cations in the monolayer. LB composition data from eight cations ( $\text{Pb}^{2+}$ ,  $\text{Cd}^{2+}$ ,  $\text{Ni}^{2+}$ ,  $\text{Co}^{2+}$ ,  $\text{Mg}^{2+}$ ,  $\text{Ca}^{2+}$ ,  $\text{Sr}^{2+}$  and  $\text{Ba}^{2+}$ ) were used in order to obtain their respective equilibrium constants. The values obtained for these constants are lower than those typically reported, which are those of short-chain carboxylic acids in solution. The model also predicts the phenomena of charge reversion on the Langmuir monolayer for certain cations at high bulk concentrations and points to possible solutions to the unwelcome X-type LB depositions based on the values of the surface electric potential.

© 2007 Elsevier B.V. All rights reserved.

**Keywords:** Langmuir–Blodgett; Non-ideal adsorption; Thin films; Electrochemical model

## 1. Introduction

Deposition of thin organic films with particular structure and functionality on solid substrates can lead to the production of components with optical, biological or electrical properties. Among the different techniques that can be used to transfer a film to a solid substrate, the Langmuir–Blodgett (LB) technique has attracted increasing attention since it allows the fabrication of precise thickness, anisotropic and perfectly ordered mono- and multilayer molecular films [1]. The LB technique consists of the vertical movement of a solid substrate upwards and downwards through a Langmuir (L) monolayer that is assembled at

the air–water interface in a Langmuir trough. The L monolayer is formed by amphiphilic molecules that are compressed to obtain a perfectly ordered arrangement of the molecules before being transferred to the solid substrate.

The classical L monolayer forming materials are long chain fatty acids and their metal salts, compounds originally used by the creators of the technique, Irving Langmuir and Katherine Blodgett [2,3]. In order to incorporate metal ions to the deposited L film (LB film), a salt of the metal cation should be added to the water subphase. The metal cation can form salts with the head groups of the amphiphilic molecule at a given pH at which the ionization of the hydrophilic group occurs. The resulting LB films are particularly interesting since they have multiple applications [1]. In particular, divalent metal ions like  $\text{Co}^{2+}$  or  $\text{Ni}^{2+}$  display magnetic properties [4], monolayers of fatty acid salts of Pb or Cd can be used as precursors for the synthesis of semiconductor nanoparticles [5–7]

*Abbreviations:* L, Langmuir; LB, Langmuir–Blodgett

\* Corresponding author. Tel.: +34 923 29 4479.

E-mail address: javimon@usal.es (F.J. Montes).

## Nomenclature

### Notation

$a$	activities of the different species in the equilibrium (dimensionless)
$A$	denominator in Eq. (4) (dimensionless)
$C_{M^{2+}}^b$	concentration of the divalent cation in the bulk liquid (mol/m <sup>3</sup> )
$C_{H^+}^b$	concentration of protons in the bulk liquid (mol/m <sup>3</sup> )
$k_B$	Boltzmann's constant ( $1.38 \times 10^{-23}$ J/K)
$K_i$	equilibrium constant for species $i$ (dimensionless)
$p$	degree of aggregation (dimensionless)
$R$	ideal Gas constant (8.31 J/mol K)
$T$	temperature (K)
$x_{M^{2+}}^b$	mole fraction of the cation in the bulk liquid (dimensionless)
$x_{H^+}^b$	mole fraction of protons in the bulk liquid (dimensionless)
$y_i$	mole fraction of the species $i$ at the interface (dimensionless)

### Greek letters

$\varepsilon$	dielectric constant of water (dimensionless)
$\varepsilon_0$	vacuum permittivity ( $8.8542 \times 10^{-12}$ F/m <sup>2</sup> )
$\chi$	Flory–Huggins binary interaction parameter (dimensionless)
$\Gamma$	number of molecules per unit area (1/m <sup>2</sup> )
$\gamma$	activity coefficient (dimensionless)
$\psi^s$	electric potential at the interface (V)

and multilayers of barium stearate present optical properties [8].

Despite the multiple applications and unique properties of LB films, a broad application of the LB technique is still not possible because what is perceived as a lack of reliability of the technique, basically due to the partial knowledge of the relationship between the feasibility of deposition and specific experimental parameters. In particular, the conditions for the successful deposition of multilayers are complex and many times, a proper analysis of the effect of different experimental variables is not possible due to missing information about important parameters in the process, such as the working pH or existing contact angles [9,10]. According to previous publications, three multilayer structures can be found [11,12]. When a monolayer is being deposited both during upstrokes and downstrokes, the resulting multilayer structure is the typical accumulation of bilayers showing the head-to-head and tail-to-tail structure described as Y-type. Many authors consider this bilayer structure as the basic, ideal stable unit of an LB film [11]. On the other hand, L monolayers may be deposited only during upstrokes or downstrokes giving as a result Z-type and X-type multilayers [11]. In practice, it is observed that the first few layers are deposited as Y-type films while after a few strokes, the film fails to deposit in one direction. This behavior is described as a Y-

type to X-type transition or as a Y-type to Z-type transition [11,13].

According to experimental results previously reported [12], the type of divalent metal ion used during the multilayer LB deposition, together with the subphase pH and the velocity of the deposition process, are decisive on the existence of transitions from Y-type to X-type multilayer deposition. Taking these facts into account, the accurate knowledge of the composition of the L and LB monolayers under particular experimental conditions would lead to the precise control of a successful LB deposition.

At least three detailed quantitative models have been proposed to predict the composition at the L monolayer at particular pH values at which the partial or total ionization of the carboxylic acid takes place. The first model is due to Bloch and Yun [14]. In their model, L monolayers of fatty acids, represented as RH (where R indicates the hydrocarbon chain of the fatty acid) exposed to water solutions of metal divalent cations ( $M^{2+}$ ) are composed of given surface concentrations of the dissociated acid ( $R^-$ ) and the intermediate charged cation ( $RM^+$ ) resulting from the adsorption of the metal divalent cation,  $M^{2+}$  on the ionized carboxylic head,  $R^-$ . The adsorption is considered to be of the Langmuir type. Later, Ahn and Franses [15] developed a model based on the argument that ionization leads just to formation of the soap ( $R_2Me$ ), rather than the intermediate compound and considered that the adsorption of the cation onto the interface is non-ideal. The third model [16] puts together a more sophisticated electrochemical approach, that considered the possibility of double layer overlapping in the meniscus region where the LB deposition takes place. In a previous paper [17], a model that considered the coexistence of all ionized and unionized species on the interface was developed. However, this model does not include the possibility of non-ideal adsorption of the metal ions on the ionized carboxylic group and describes this process based on the Langmuir isotherm.

The present study aims to unify previous models that describe only partially the experimentally observed L monolayer composition. The model includes the consideration of all possible ionized and unionized species on the interface (RH,  $R^-$ ,  $RM^+$  and  $R_2M$ ) together with a modified Langmuir isotherm accounting for the non-ideal adsorption of ions and a geometry consisting of a flat charged monolayer adjacent to a semi-infinite volume of electrolyte solution. As an added feature and based on experimental data, the model allows the calculation of the equilibrium constants for the formation of the  $RM^+$  and  $R_2Me$  complexes of insoluble long-chain carboxylic acids. The values of these constants have been previously taken from soluble short-chain carboxylic acid complexes [14], introducing in some cases certain degree of indetermination in the results. Eight different divalent metal cations are considered in this study ( $Pb^{2+}$ ,  $Cd^{2+}$ ,  $Ni^{2+}$ ,  $Co^{2+}$ ,  $Mg^{2+}$ ,  $Ca^{2+}$ ,  $Sr^{2+}$  and  $Ba^{2+}$ ). The computational results obtained from the developed model regarding RH concentrations and system pKa show an excellent agreement with experimental results. Moreover, the obtained values of the equilibrium constants for the formation of  $RM^+$  and  $R_2Me$  are lower than those reported [18] for short-chain carboxylic acids, as it should be expected.

## 2. Theoretical model

The model presented here has three main considerations. First, it is based on the chemical equilibrium between the different species that can be eventually formed between a dissociated long-chain carboxylic acid ( $R^-$ ) and a divalent cation ( $M^{2+}$ ). Second, it takes into account the non-ideal interactions among  $M^{2+}$  and  $H^+$  present in the subphase. Following the scheme presented elsewhere [15], the fully dissociated monolayer is considered to be a lattice structure of vacant sites where the  $H^+$  and the  $M^{2+}$  can be adsorbed. The non-ideal behavior of the adsorption process comes from the assumption that the adsorption of one ion (p.e.  $M^{2+}$ ) at a vacant site is affected by the presence of an equal (another  $M^{2+}$ ) or a different ( $H^+$ ) ion in the neighboring sites. Under this premise, the Langmuir isotherm will not be adequate to model the adsorption process. Finally, the third consideration accounts for the electrochemical description of the system. This consists of a flat charged monolayer adjacent to a semi-infinite volume of electrolyte solution. The charge density of the monolayer is the result of the unbalance of electrical charges generated by the different concentrations of the positively and negatively charged species. Those concentrations are determined by the chemical equilibrium and the non-ideal adsorption of the cations at the interface. Consequently, a different surface potential is generated on the monolayer for the different divalent cations. This potential may be responsible for the successful (Y-type) or unsuccessful (X-type) deposition of multiple LB structures on solid substrates [12,17].

### 2.1. Chemical equilibrium

The chemical equations accounting for all the species present in the Langmuir monolayer are:



Consequently, the activities of the different species on the monolayer as a function of the activity of the dissociated acid ( $a_{R^-}$ ) are:

$$\begin{aligned} a_{RH} &= K_H a_{R^-} a_{H^+}^s \\ a_{R_2M} &= K_{R_2M} (a_{R^-})^2 a_{M^{2+}}^s \\ a_{RM^+} &= K_{RM^+} a_{R^-} a_{M^{2+}}^s \end{aligned} \quad (2)$$

$a_{Me^{2+}}^s$  and  $a_{H^+}^s$  are the surface concentrations of cation and protons.

### 2.2. Non-ideal adsorption onto the Langmuir monolayer

One objective of the model is to obtain the values of the fractional condensations ( $F_i$ ) of the different species adsorbed in the monolayer in order to determine the subsequent composition of the LB films. As it is described by other authors [15], using an analogy between a 2D and a 3D lattice model, the fractional con-

denation ( $F_i$ ) or area fraction of the  $i$ -species in the monolayer is:

$$F_i = \frac{p_i y_i}{\sum_{i=1}^N p_i y_i} \quad (3)$$

In Eq. (3),  $p_i$  is the degree of aggregation of the  $i$ -species with respect to the fatty acid chain R ( $p_{RH} = p_{RMe^+} = p_{R^-} = 1$  and  $p_{R_2M} = 2$ ).  $N$  is the total number of chemical species in the Langmuir monolayer ( $N=4$  in our case:  $RH$ ,  $R^-$ ,  $RM^+$  and  $R_2M$ ) and  $y_i$  is the mole fraction of the  $i$ -species.

Using Eq. (3) the fractional condensations of the components at the monolayer are:

$$\begin{aligned} F_{R^-} &= \frac{y_{R^-}}{y_{R^-} + y_{RH} + 2y_{R_2M} + y_{RM^+}} \\ &= \frac{1}{1 + y_{RH}/y_{R^-} + 2y_{R_2M}/y_{R^-} + y_{RM^+}/y_{R^-}} = \frac{1}{A} \\ F_{RH} &= \frac{y_{RH}}{y_{R^-} + y_{RH} + 2y_{R_2M} + y_{RM^+}} = \frac{y_{RH}/y_{R^-}}{A} \\ F_{R_2M} &= \frac{y_{R_2M}}{y_{R^-} + y_{RH} + 2y_{R_2M} + y_{RM^+}} = \frac{y_{R_2M}/y_{R^-}}{A} \\ F_{RM^+} &= \frac{y_{RM^+}}{y_{R^-} + y_{RH} + 2y_{R_2M} + y_{RM^+}} = \frac{y_{RM^+}/y_{R^-}}{A} \end{aligned} \quad (4)$$

Activities are related to the molar fractions of each species by an activity coefficient  $\gamma_i$ :

$$a_i = \gamma_i y_i \quad (5)$$

Using the relations included in Eqs. (2) and (5), the denominator  $A$  of Eq. (4) becomes:

$$\begin{aligned} A &= 1 + K_H a_{H^+}^s \left( \frac{\gamma_{R^-}}{\gamma_{RH}} \right) + 2K_{R_2M} a_{M^{2+}}^s \left( \frac{(\gamma_{R^-})^2 \gamma_{R^-}}{\gamma_{R_2M}} \right) \\ &\quad + K_{RM^+} a_{M^{2+}}^s \left( \frac{\gamma_{R^-}}{\gamma_{RM^+}} \right) \end{aligned} \quad (6)$$

The non-ideal adsorption features of the system are taken care of using the Flory–Huggins interaction parameters  $\chi_{ij}$ , which reflect the intensity of the binary interactions between the species contained at the monolayer. In the present model, just the parameter related to the interaction of species containing protons and divalent cations is considered. The relation between the activities and the fractional condensations of the different species at the interface is [15]:

$$\begin{aligned} \ln \left( \frac{a_i}{F_i} \right) &= \left[ \sum_{j \neq i} \left( 1 - \frac{p_j}{p_i} \right) F_j \right] + p_i \left[ \left( (1 - F_i) \sum_{j \neq i} \chi_{ij} F_j \right) \right. \\ &\quad \left. - \frac{1}{2} \left( \sum_{j \neq i} \sum_{k \neq j} \chi_{jk} F_j F_k \right) \right] \end{aligned} \quad (7)$$

Table 1  
Experimental and theoretical values of several parameters related to the model

Metal	$K_{R_2M}$ (model) <sup>a</sup>	$K_{RM^+}$ (model) <sup>a</sup>	$\chi^b$	$pK_a$ (exp) <sup>c</sup>	$pK_a$ (model)	Pauling electronegativity	$K_{R_2M}$ (experimental) <sup>d</sup>	$K_{RM^+}$ (experimental) <sup>d</sup>
Pb	$2.5 \times 10^6$	$1.4 \times 10^3$	0.78	4.1	4.1	2.3	$4.4 \times 10^7$	$2.4 \times 10^4$
Cd	$6.7 \times 10^3$	22.5	0.13	5.6	5.5	1.7	$2.9 \times 10^5$	$9.9 \times 10^2$
Ni	0.94	0.01	0.4	7.5	7.5	1.9	$2.2 \times 10^4$	$2.9 \times 10^2$
Co	2.73	0.03	0.4	7.1	7.3	1.9	$2.0 \times 10^4$	$2.3 \times 10^2$
Mg	$\approx 0$	10.2	-0.2	6.8	6.9	1.3	$\approx 0$	$1.9 \times 10^2$
Ca	$\approx 0$	22.7	-0.76	6.7	6.7	1.0	$\approx 0$	$1.8 \times 10^2$
Sr	$\approx 0$	22.9	-1	6.9	6.7	0.9	$\approx 0$	$1.3 \times 10^2$
Ba	$\approx 0$	13.3	-4.1	6.9	6.8	0.9	$\approx 0$	$1.1 \times 10^2$

Bulk cation concentration is 0.1 mM for all cations except for Ni and Co, for which  $C_{M^{2+}}^b = 0.03$  mM.

<sup>a</sup> The values of  $K$  correspond to long chain carboxylic acids, for example, stearic acid (C<sub>18</sub>).

<sup>b</sup> Values of the Flory–Huggins interaction parameters interpolated using values of Pauling electronegativity.

<sup>c</sup> Experimental values of  $pK_a$  are taken from: Pb [21]; Cd and Ba [20]; Ni and Co [4]; Mg and Sr [24]; Ca [29].

<sup>d</sup> Experimental values of  $K_{R_2M}$  and  $K_{RM^+}$  for short-chain carboxylic acids (propanoic acid (C<sub>3</sub>)) are taken from Martell [18].

Combining Eqs. (5) and (7) for each adsorbed component at the interface yields:

$$\begin{aligned} \ln \left( \frac{\gamma_{R^-} \gamma_{R^-}}{F_{R^-}} \right) &= \frac{F_{R_2M}}{2} - (\chi F_{RH})(F_{R_2M} + F_{RM^+}) \\ \ln \left( \frac{\gamma_{RH} \gamma_{RH}}{F_{RH}} \right) &= \frac{F_{R_2M}}{2} - \chi(1 - F_{RH})(F_{R_2M} + F_{RM^+}) \\ \ln \left( \frac{\gamma_{R_2M} \gamma_{R_2M}}{F_{R_2M}} \right) &= -(F_{R^-} + F_{RH} + F_{R_2M}) \\ &\quad + 2[(\chi F_{RH})(1 - F_{R_2M} - F_{RM^+})] \\ \ln \left( \frac{\gamma_{RM^+} \gamma_{RM^+}}{F_{RM^+}} \right) &= \frac{F_{R_2M}}{2} + [(\chi F_{RH})(1 - F_{R_2M} - F_{RM^+})] \end{aligned} \quad (8)$$

Determination of the fractional condensations ( $F_i$ ) using Eq. (4) requires the previous calculation of the factors  $(\gamma_{R^-}/\gamma_{RH})$ ,  $((\gamma_{R^-})^2 \gamma_{R^-}/\gamma_{R_2M})$  and  $(\gamma_{R^-}/\gamma_{RM^+})$  using the relationships included in Eq. (8). In this way, the values of  $F_i$  will depend on the Flory–Huggins interaction parameter  $\chi$  accounting for the non-ideal adsorption. After some algebra, one gets:

$$\begin{aligned} \left( \frac{\gamma_{R^-}}{\gamma_{RH}} \right) &= e^{-\chi(F_{R_2M} + F_{RM^+})} \\ \left( \frac{(\gamma_{R^-})^2 \gamma_{R^-}}{\gamma_{R_2M}} \right) &= \left( \frac{F_{RH}}{K_H a_{H^+}^s} \right) e^{(1 + \chi)(F_{R_2M} + F_{RM^+} - 2F_{RH})} \\ \left( \frac{\gamma_{R^-}}{\gamma_{RM^+}} \right) &= e^{-\chi F_{RH}} \end{aligned} \quad (9)$$

### 2.3. Electrochemical description of the system

The unbalance of electrical charges at the interface generated by the concentration difference of the charged species results in a surface charge density that can be calculated by Eq. (10).

$$\sigma = -q\Gamma(F_{R^-} - F_{RM^+}) \quad (10)$$

Considering the so-called “flat approximation” in which a single flat charged plane is bounded by a semi-infinite volume of an electrolyte solution [16], the Poisson–Boltzmann equation is solved to give an analytical expression relating the surface charge density at the flat plane ( $\sigma$ ) with the electric potential at

the interface ( $\psi^s$ ):

$$\begin{aligned} \sigma &= (1 - e^{-(q\psi^s/k_B T)})[2\varepsilon\varepsilon_0 RT(C_{M^{2+}}^b \\ &\quad + (C_{H^+}^b + 2C_{M^{2+}}^b) e^{-(q\psi^s/k_B T)})] \end{aligned} \quad (11)$$

$C_{M^{2+}}^b$  and  $C_{H^+}^b$  are the molar concentrations of divalent cation and protons in the bulk liquid, which are part of the experimental conditions. Connecting Eqs. (10) and (11) results in the Grahame equation [19] for this specific configuration:

$$\begin{aligned} -q\Gamma(F_{R^-} - F_{RM^+}) &= (1 - e^{-(q\psi^s/k_B T)})[2\varepsilon\varepsilon_0 RT(C_{M^{2+}}^b \\ &\quad + (C_{H^+}^b + 2C_{M^{2+}}^b) e^{-(q\psi^s/k_B T)})] \end{aligned} \quad (12)$$

The activities of protons ( $a_{H^+}^s$ ) and divalent cation ( $a_{M^{2+}}^s$ ) at the interface are calculated based on the activities in the bulk liquid and on the value of the electric potential at the interface:

$$\begin{aligned} a_{H^+}^s &= a_{H^+}^b e^{-(q\psi^s/k_B T)} \\ a_{M^{2+}}^s &= a_{M^{2+}}^b e^{-2(q\psi^s/k_B T)} \end{aligned} \quad (13)$$

Activities of protons and cations at the surface can be approximated to the molar fractions at the surface, as it has been previously done [15]. Then,  $a_{H^+}^s \approx x_{H^+}^s$ , and  $a_{M^{2+}}^s \approx x_{M^{2+}}^s$ .

Relations (4) and (12) conform a system of five non-linear algebraic equations with five unknowns [ $F_{R^-}$ ,  $F_{RH}$ ,  $F_{RM^+}$ ,  $F_{R_2M}$  and  $\psi^s$ ] that are solved by an iterative procedure implemented in Matlab<sup>®</sup>. Previously, some parameters of the model ( $K_H$ ,  $K_{R_2M}$ ,  $K_{RM^+}$  and  $\chi$ ) must be evaluated. Details about the procedure leading to the calculation of those parameters are given in the next section. The values obtained are summarized in Table 1.

## 3. Results and discussion

### 3.1. Determination of experimental constants

$K_H$  is the dimensionless dissociation constant for the carboxylic acid and is equal to  $3.63 \times 10^6$ , the value of the soluble short-chain carboxylic acids (propanoic and butanoic acids) [18]. It is considered that there is not appreciable change in the dissociation constant as the length of the carboxylic acid

increases. This assumption has been broadly accepted by different authors [14,15,20].

The Flory–Huggins interaction parameter ( $\chi$ ) has been previously determined [15] for four divalent cations (Pb, Cd, Ca, Ba). Moreover, the authors found an experimental relationship between  $\chi$  and the electronegativity of each cation. This relationship is used in the present paper to interpolate the values of  $\chi$  for the rest of the cations under study (Ni, Co, Mg, Sr). The results obtained are presented in Table 1.

The values of  $K_{R_2M}$  and  $K_{RM^+}$  are obtained simultaneously during the procedure of solving the system of five non-linear algebraic equations given by relations (4) and (12). Experimental data of RH concentrations on LB films are fitted to the theoretical

RH concentrations given by the model. A least square routine is used for such purpose. At this point, it is considered that the theoretical concentration of RH in the Langmuir monolayer is translated without change to the LB film. Giving the problems derived from trying to fit too many parameters at the same time, just  $K_{RM^+}$  is directly obtained by fitting the experimental data. Calculation of  $K_{R_2M}$  assumes that the ratio  $K_{R_2M}/K_{RM^+}$  remains the same as the ratio presented in bibliography [18] for short-chain carboxylic complexes of the same cations. The obtained results of  $K_{RM^+}$  and  $K_{R_2M}$  are summarized in Table 1. Experimental RH concentration data are taken from [21] (Pb, Cd, Ca, Ba), [22] (Cd, Ca, Ba), [23] (Cd), [4] (Ni, Co) and [24] (Mg).

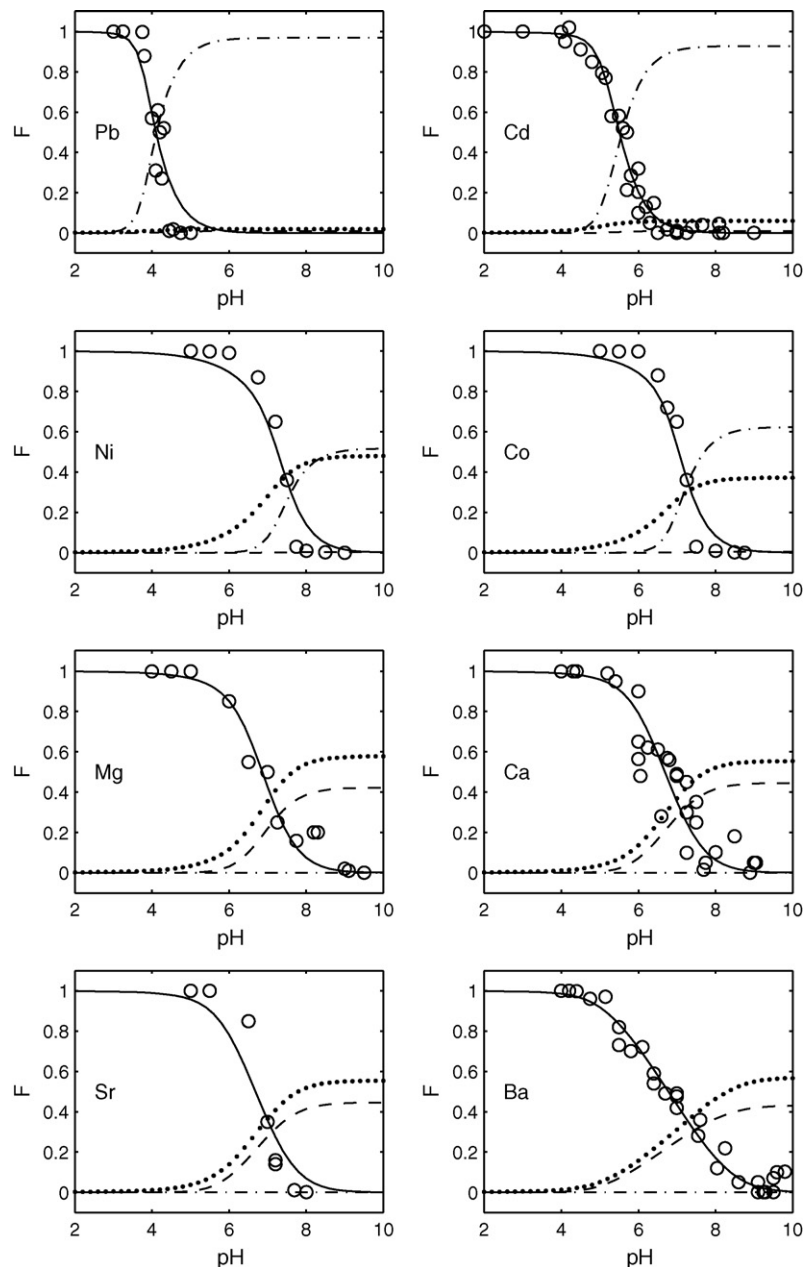


Fig. 1. Theoretical fractional condensations ( $F$ ) of all species present at the interface for the cations under study as a function of pH: solid line ( $F_{RH}$ ); dotted line ( $F_{R^-}$ ); dashed line ( $F_{RM^+}$ ); dash-dot line ( $F_{R_2M}$ ); circles (experimental values of  $F_{RH}$ ). Bulk cation concentration is 0.1 mM.

### 3.2. Comments on the values of the equilibrium constants and on the influence of pH, cation type and cation concentration on the LB deposition process

Fig. 1 shows the theoretical results obtained from the model regarding the fractional condensations ( $F$ ) of all the species present at the interface together with the experimental values of  $F_{RH}$  (circles). The model reproduces within good limits of approximation the experimental values of ( $F_{RH}$ ). It seems pretty reasonable to think that the values of  $K_{R_2M}$  for the long-chain insoluble carboxylic salts must be smaller than those reported [18] for short-chain soluble salts. In some cases (Mg, Ca, Sr, Ba)  $K_{R_2M}$  is zero for short-chain soluble salts, which means they should also be zero for the long-chain insoluble carboxylic salts. The results of the model corroborate this fact (see Table 1) in opposition to previous results [15] for Ca and Ba, where the values of  $K_{R_2M}$  for long-chain carboxylic salts are higher than the reported values of  $K_{R_2M}$  for short-chain carboxylic salts. This flaw comes from assuming that just the salt can be formed at the interface, not allowing for the formation of the intermediate complex  $RM^+$ .

Values of  $K_{RM^+}$  obtained by the model agree well with our expectations, being also lower than the values reported for short-chain carboxylic acids (see Table 1).

It has been experimentally established [10,25,26] that the  $pK_a$  of the system is a characteristic pH at which important transitions among different type of LB depositions take place and where the stability of the Langmuir monolayer is maximum [27]. The  $pK_a$  is defined as the bulk pH at which the carboxylic acid is 50% ionized ( $F_{RH}=0.5$ ). Experimental values of  $pK_a$  for different

cations are reported in the literature [28–30]. In this context, it is of great interest to compare the theoretical  $pK_a$  predictions of the model with the experimental data available. The model predictions are pretty accurate (see Table 1), providing an interesting practical applicability regarding the prediction of the optimal pH for the successful LB deposition of any divalent cation.

Fig. 2 presents the values of the surface electric potential versus bulk pH for the eight cations under study. It is interesting to point out that the change in the slope of the curves coincides with the  $pK_a$  of each cation. This fact provides a way of predicting experimental  $pK_a$  values by measuring the electric potential at the interface. Another interesting observation is that the lower the absolute value of the surface potential of the cation (p.e. Pb) at  $pH=pK_a$  (optimal LB deposition conditions), the higher the possibility of having an X-type LB deposition. During the X-type mechanism, the deposition is only successful when the solid moves upwards from the liquid, in contrast to the Y-type, where layers are deposited both in the way up and down. This is one of the main disadvantages of the LB technique and most experimental efforts intend to avoid this problem [12]. Then, it looks like the optimization of the experimental conditions for LB depositions should account for this variable, trying to maximize the absolute value of the surface potential. In this context, increasing the solid dipping speed increases the chances of having a Y-type deposition [12], probably due to a transient increase in the absolute value of the surface potential, as a result of a short-period perturbation hydrodynamically induced in the electrical double layer.

Fig. 3 shows the values of surface electric potential as a function of the bulk pH at four different bulk cation concentrations

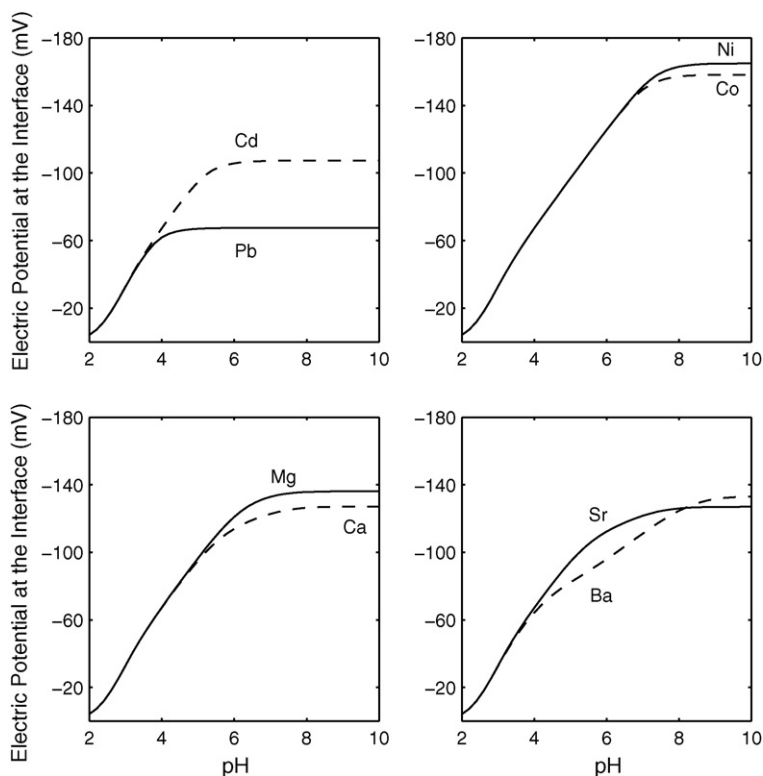


Fig. 2. Surface electric potential as a function of the bulk pH for eight divalent cations. Bulk cation concentration is 0.1 mM.

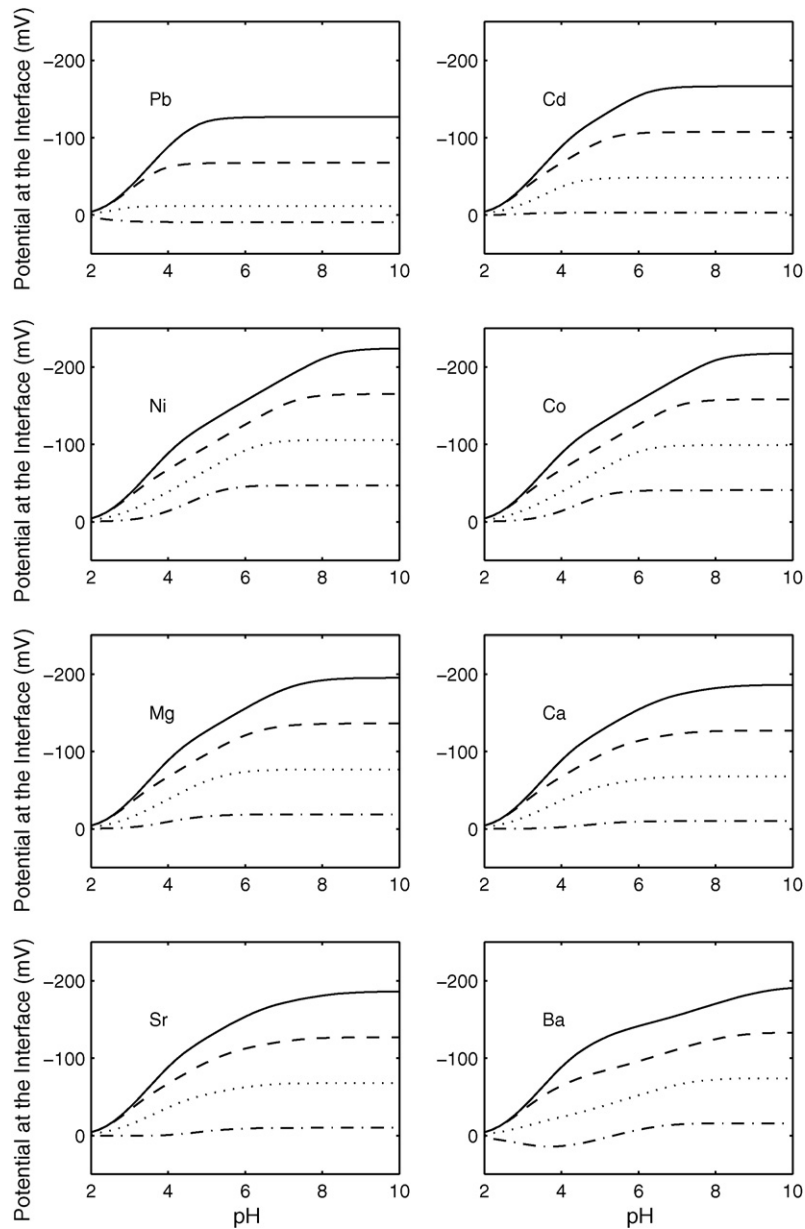


Fig. 3. Surface electric potential as a function of the bulk pH at four different bulk cation concentrations: solid line ( $C_{M^{2+}}^b = 10^{-3}$  mM); dashed line ( $C_{M^{2+}}^b = 10^{-1}$  mM); dotted line ( $C_{M^{2+}}^b = 10$  mM); dash-dot line ( $C_{M^{2+}}^b = 10^3$  mM).

for the eight cations under study. This theoretical study tries to demonstrate whether it is possible to revert the charge of the Langmuir monolayer (switching from negative to positive) when the bulk cation concentration ( $C_{M^{2+}}^b$ ) is sufficiently high. Although we did not experimentally test it, charge reversion phenomena has been reported in some biological systems [31] and this is one of the arguments for including the formation of the intermediate  $RM^+$  in the system of equations accounting for the chemical equilibrium [14]. According to the theoretical curves shown in Fig. 3, charge reversion is possible for systems containing Pb for the whole range of pH when  $C_{Pb^{2+}}^b \geq 1$  M and for Ba at low pH and also  $C_{Ba^{2+}}^b \geq 1$  M.

Fig. 3 also shows that the absolute value of the surface potential increases when  $C_{M^{2+}}^b$  decreases. This feature is interesting

because it points to a possible solution for the unwelcome X-type LB depositions found when using, for example, Pb at low dipping speeds and the standard  $C_{Pb^{2+}}^b = 0.1$  mM. Actually, it has been reported [32,33] successful Y-type depositions for Pb at  $C_{Pb^{2+}}^b = 0.03$  mM. This fact would confirm that higher negative values of the surface potential benefit the possibility of having Y-type LB depositions.

#### 4. Conclusions

An electrochemical model has been developed to improve and complete previous efforts in predicting the composition of Langmuir monolayers of divalent cations adsorbed onto a surface containing a long-chain carboxylic acid. The model constitutes

an useful tool for optimizing the process of depositing multiple Langmuir–Blodgett films on a solid substrate. Besides other features, the model allows a realistic calculation of the equilibrium constants for the formation of the complexes between the carboxylic acid and the divalent cation based on a compilation of experimental data regarding the composition of the subsequent LB films. In contrast with previous models, the present model does not constraint the possibility of the formation of both the complexes containing one and/or two molecules of acid on the surface of the original Langmuir monolayer and it includes the non-ideal mixing behavior of the cations in the monolayer. LB composition data from eight divalent cations were used in order to obtain their respective equilibrium constants. The theoretical values obtained for these constants are lower than the data typically reported, which usually refers to short-chain carboxylic acids in solution. The model also predicts the phenomena of charge reversion on the Langmuir monolayer for certain cations at high bulk concentrations and points to possible solutions to the unwelcome X-type LB depositions observed for some cations at low dipping speeds.

### Acknowledgements

This research was performed under a grant from the Junta de Castilla-León (Spain), SA022B06.

### References

- [1] G.G. Roberts, Langmuir–Blodgett Films, Plenum Press, 1990.
- [2] I. Langmuir, The constitution and fundamental properties of solids and liquids. II. Liquids, *J. Am. Chem. Soc.* 39 (1917) 1848–1906.
- [3] K.B. Blodgett, Films built by depositing successive monomolecular layers on a solid surface, *J. Am. Chem. Soc.* 57 (1935) 1007–1022.
- [4] Y. Ando, T. Hiroike, T. Miyashita, T. Miyasaki, Magnetic properties of stearate films with 3D transition metal ions fabricated by the Langmuir–Blodgett method, *Thin Solid Films* 278 (1996) 144–149.
- [5] A.V. Nabok, A.K. Ray, A.K. Hassan, J.M. Titchmarsh, F. Davis, T. Richardson, A. Starovoitov, S. Bayliss, Formation of CdS nanoclusters within LB films of calixarene derivatives and study of their size-quantization, *Mater. Sci. Eng. C: Biomimetic Supramol. Syst.* 8–9 (1999) 171–177.
- [6] V. Erokhin, L. Feigin, G. Ivakin, V. Klechkovskaya, Y. Lvov, N. Stiopina, Formation and X-ray and electron-diffraction study of Cds and Pbs particles inside fatty-acid matrix, *Makromol. Chem.: Macromol. Symp.* 46 (1991) 359–363.
- [7] E.S. Smotkin, C. Lee, A.J. Bard, A. Campion, M.A. Fox, T.E. Mallouk, S.E. Webber, J.M. White, Size quantization effects in cadmium-sulfide layers formed by a Langmuir–Blodgett technique, *Chem. Phys. Lett.* 152 (1988) 265–268.
- [8] K.B. Blodgett, I. Langmuir, Built-up of barium stearate and their optical properties, *Phys. Rev. A* 51 (1937) 964–982.
- [9] R.L. Cerro, Moving contact lines and Langmuir–Blodgett film deposition, *J. Colloid Interface Sci.* 257 (2003) 276–283.
- [10] M.E. Díaz, R.L. Cerro, On the effect of subphase pH and counterions on transfer ratios and dynamic contact angles during deposition of multiple Langmuir–Blodgett monolayers, *Thin Solid Films* 485 (2005) 224–229.
- [11] D.K. Schwartz, Langmuir–Blodgett film structure, *Surf. Sci. Rep.* 27 (1997) 241–334.
- [12] M.E. Díaz, R.L. Cerro, Surface potentials and ionization equilibrium in Y-type deposition of multiple Langmuir–Blodgett films. I. Effect of pH and counterions, *J. Colloid Interface Sci.* 285 (2005) 686–693.
- [13] G.L. Gaines, Insoluble Monolayers at Gas Liquid Interfaces, Interscience Monographs in Physical Chemistry, John Wiley & Sons, 1966.
- [14] J.M. Bloch, W.B. Yun, Condensation of monovalent and divalent metal-ions on a Langmuir monolayer, *Phys. Rev. A* 41 (1990) 844–862.
- [15] D.J. Ahn, E.I. Franses, Interactions of charged Langmuir monolayers with dissolved ions, *J. Chem. Phys.* 95 (1991) 8486–8493.
- [16] V.I. Kovalchuk, E.K. Zholkovskiy, N.P. Bondarenko, D. Vollhardt, Dissociation of fatty acid and counterion binding at the Langmuir monolayer deposition: theoretical considerations, *J. Phys. Chem. B* 105 (2001) 9254–9265.
- [17] M.E. Díaz, F.J. Montes, R.L. Cerro, Surface potentials and ionization equilibrium in Y-type deposition of multiple Langmuir–Blodgett films. II. Theoretical model, *J. Colloid Interface Sci.* 285 (2005) 694–702.
- [18] A.E. Martell, R.M. Smith, Critical Stability Constants: Other Organic Ligands, vol. 3, Plenum Press, 1977.
- [19] D.C. Grahame, The electrical double layer and the theory of electrocapilarity, *Chem. Rev.* 41 (1947) 441–501.
- [20] J.G. Petrov, I. Kuleff, D. Platikanov, Neutron-activation analysis of metal-ions in Langmuir–Blodgett multilayers of arachidic acid, *J. Colloid Interface Sci.* 88 (1982) 29–35.
- [21] K. Kobayashi, K. Takaoka, Application of X-ray photoelectron-spectroscopy and Fourier-transform IR-reflection absorption-spectroscopy to studies of the composition of Langmuir–Blodgett films, *Thin Solid Films* 159 (1988) 267–273.
- [22] J.G. Petrov, K. Ivelin, D. Platikanov, Neutron activation analysis of metal ions in Langmuir–Blodgett multilayers of arachidic acid, *J. Colloid Interface Sci.* 88 (1981) 29–35.
- [23] J.G. Petrov, H. Kuhn, D. Mobius, 3-Phase contact line motion in the deposition of spread monolayers, *J. Colloid Interface Sci.* 73 (1980) 66–75.
- [24] D.W. Deamer, D.W. Meek, D.G. Cornwell, Properties composition and structure of stearic acid-stearate monolayers on alkaline earth solutions, *J. Lipid Res.* 8 (1967) 255–263.
- [25] R. Aveyard, B.P. Binks, P.D.I. Fletcher, X. Ye, Contact angles and transfer ratios measured during the Langmuir–Blodgett deposition of docosanoic acid onto mica from CdCl<sub>2</sub> subphases, *Colloids Surf. A: Physicochem. Eng. Aspects* 94 (1995) 279–289.
- [26] R. Aveyard, B.P. Binks, P.D.I. Fletcher, X. Ye, Dynamic contact angles and deposition efficiency for transfer of docosanoic acid on to mica from CdCl<sub>2</sub> subphases as a function of pH, *Thin Solid Films* 210 (1992) 36–38.
- [27] R. Aveyard, B.P. Binks, A.W. Cross, P.D.I. Fletcher, Dicarboxylic acids: stability of insoluble monolayers and ionisation in Langmuir–Blodgett multilayers, *Colloids Surf. A: Physicochem. Eng. Aspects* 98 (1995) 83–91.
- [28] B.P. Binks, Insoluble monolayers of weakly ionizing low molar mass materials and their deposition to form LB multilayers, *Adv. Colloid Interface Sci.* 34 (1991) 343–432.
- [29] R. Aveyard, B.P. Binks, N. Carr, A.W. Cross, Stability of insoluble monolayers and ionization of Langmuir–Blodgett multilayers of octadecanoic acid, *Thin Solid Films* 188 (1990) 361–373.
- [30] A. Dhanabalan, N.P. Kumar, S. Major, S.S. Talwar, Variation of monolayer behaviour and molecular packing in zinc arachidate LB films with subphase pH, *Thin Solid Films* 329 (1998) 787–791.
- [31] S. McLaughlin, N. Mulrine, T. Gresalfi, G. Vaio, A. McLaughlin, Adsorption of divalent-cations to bilayer-membranes containing phosphatidylserine, *J. Gen. Physiol.* 77 (1981) 445–473.
- [32] M.W. Charles, Optimization of multilayer soap crystals for ultrasoft X-ray diffraction, *J. Appl. Phys.* 42 (1971) 3329–3356.
- [33] W. Mahler, T.A. Barberka, U. Pietsch, U. Hohne, H.J. Merle, Thermally-induced phase-transitions in LB multilayers of lead stearate, *Thin Solid Films* 256 (1995) 198–204.